Proceedings of the International Symposium of Mechanism and Machine Science, 2017
AzC IFToMM – Azerbaijan Technical University
11-14 September 2017, Baku, Azerbaijan

Kinematic analysis of the 3-RPS manipulator using the geometry of plane curves

Sandipan BANDYOPADHYAY[1*], Teja Krishna MAMIDI[2], Aravind BASKAR[3]

[1*]Assistant Professor
Department of Engineering Design
Indian Institute of Technology Madras
Chennai 600 036
e-mail: sandipan@iitm.ac.in

[2]Research Scholar
e-mail: tejaiiit27@gmail.com

[3]Research Scholar
e-mail: krishna.arvind91@gmail.com

Abstract
This paper reports a number of interesting observations regarding the kinematics and singularities of a spatial parallel manipulator, namely, the 3-RPS manipulator. It is well known in literature that the manipulator has two operation modes. Recently, it was shown that the forward kinematic problem of the manipulator is equivalent to the intersection of a circle with a pair of quad-circular octic curves, corresponding to the two operation modes, in the plane of the said circle. In this work, some special points of these octic curves are analysed and corroborated against the singularities of the manipulator. The transition between the modes are also examined from the perspective of the intersection of the octic curves. Finally, the conditions leading to finite self motions of the manipulator are derived and validated against those in the existing literature. The method of analysis is intuitive, simple, and at the same time, quite capable of retrieving existing results, as well as deriving fresh ones.

Keywords: 3-RPS manipulator, Singularity, Finite self-motion, Double point, Quad-circular octic curve

1. Introduction

In the study of kinematics of manipulators one often encounters *circular* curves. One of the most famous examples of this is the coupler-curve of the planar four-bar mechanism, which is perhaps the most well-known *tri-circular* sextic in existence, and deserves a catalogue of its own [1]. The curve reappears in the problem of forward kinematics of planar parallel manipulators, where the problem reduces to the intersection of a circle with a tri-circular sextic curve [2]. Recently, a new circular curve has been associated with the forward kinematics of a spatial manipulator, namely, the 3-RPS manipulator. It was shown in [3], that all the poses of the manipulator (for a given set of inputs) correspond to the points of intersection of a circle with a *quad-circular octic* curve in the plane of the said circle. Such a reduction of the forward kinematic problem affords a unique geometric understanding, from the perspective of the geometry of plane curves, which have been documented exhaustively in many classical works, e.g. [4].

Armed with these known results, this work tries to investigate the special geometric conditions that may occur, and the kinematic consequences thereof. In particular, this work looks at the special points of intersection, which covers the tangency of the octic curve with the circle, and the double points in the octic curve itself, which coincide with the point of intersection with the circle. It is interesting to note that while all of these cases lead to the merger of the roots of the *forward kinematic univariate* (FKU) (see [5] for a discussion on the FKU of this manipulator), not all of them are associated with the kinematic singularities of the manipulator. In other words, an interesting question emerges from these observations: "When does the (geometric) singularity of the constraint curves lead to a (kinematic) manipulator, and when does it not?" Only a rigorous analytical study can answer that question in a comprehensive manner. While that is out of scope of this paper, it does document a number of interesting situations, relating to the tangency condition, as well as the three possible types of double points, namely: the cusp, the crunode, and the acnode. At each of these situations, the following geometric/algebraic/kinematic conditions are studied, with an attempt towards correlating these conditions: the formal algebraic condition for the $\mathbf{\Sigma}^1$ singularity[1] of the manipulator, as given in [7] (henceforth referred to simply as the "singularity"); the geometric condition for the case 2 of the singularity reported in [8]; the coplanarity of one of the legs with the moving platform (as shown in an example in [5]); the condtion for obtaining a double root of the FKU, derived in terms of the Stüdy parameters in this work. The study and the results thereof are by no means complete, or conclusive. They are presented here to document a few possibilities, as hinted by the numerical examples, which need to be either proven or dismissed formally through rigorous analytical studies in the future.

The rest of the paper is oragnised as follow: the geometry and the forward kinematics problem of the 3-RPS manipulator are presented in Section 2. The intersections of the octic curves with the circle at the special points, and the kinematic consequences thereof are studied via numerical examples in Section 3. A special case where the manipulator exhibits finite self-motion is discussed in Section 4, and the results are summarised in Section 5.

[1]According to Thom-Boardman classification of singularities of a differential map f, a point x belongs to the class $\mathbf{\Sigma}^n$ if the kernel of $Df(x)$, (i.e., the differential of f at x) is of dimension n [6].

2. Geometry and kinematics of the 3-RPS manipulator

The 3-RPS manipulator has three RPS-chains, each connected at a vertex of the fixed platform $\boldsymbol{b}_1\boldsymbol{b}_2\boldsymbol{b}_3$ by a rotary joint, and to the moving platform $\boldsymbol{p}_1\boldsymbol{p}_2\boldsymbol{p}_3$, by a spherical joint, as depicted in Fig. 1. The fixed and moving platforms are equilateral triangles of circumradius b and a, respectively. A fixed frame of reference $\{A\}$, given by $\boldsymbol{o}_A$-$\boldsymbol{X}_A\boldsymbol{Y}_A\boldsymbol{Z}_A$, and a moving frame of reference $\{B\}$, given by $\boldsymbol{o}_B$-$\boldsymbol{X}_B\boldsymbol{Y}_B\boldsymbol{Z}_B$, are attached to the centroids of the fixed and the moving platforms, respectively. The actuated prismatic joint variables $\boldsymbol{l} = [l_1, l_2, l_3]^\top$ and the passive rotary joint variables $\boldsymbol{\phi} = [\phi_1, \phi_2, \phi_3]^\top$ constitute the *configuration space* of the manipulator. The forward kinematic (FK) problem of the 3-RPS manipulator is to determine the pose of the moving platform $\boldsymbol{p}_1\boldsymbol{p}_2\boldsymbol{p}_3$, for a given set of inputs $\boldsymbol{l}$. The problem can be addressed by hypothetically breaking the 3-RPS manipulator into two kinematic chains, and then finding the conditions for the two chains to close simultaneously. It can be done by removing one of the spherical joints, as shown in [3]. For instance, if the spherical joint at $\boldsymbol{p}_1$ is removed, a spatial RSSR closed chain is obtained, along with an open RP planar chain, as shown in Fig. 2. The point $\boldsymbol{p}_{s_1}$ of the RSSR-chain and the point $\boldsymbol{p}_{c_1}$ of the RP-chain coincide at the point $\boldsymbol{p}_1$ to form the 3-RPS manipulator shown in Fig. 1. By casting these geometric conditions in terms of equations and subsequently solving them, the unknown variable $\boldsymbol{\phi}$ can be obtained. The details of the process are given in [3]. The key points relevant to the present work are:

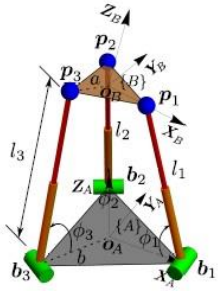

Fig. 1: Schematic of the 3-RPS manipulator

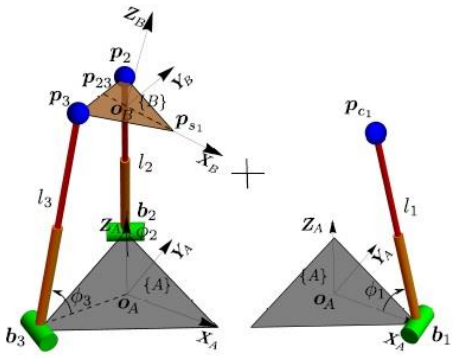

Fig. 2: Kinematic sub-chains of the 3-RPS manipulator

1. The surface traced by the point $\boldsymbol{p}_{s_1}$ of the RSSR-chain, when intersected by the plane of the RP chain forms the curve $\alpha(x,z) = 0$, where $\alpha(x,z)$ decomposes into the following factors:

$$\alpha(x,z) = \beta(x,z)O_1(x,z)O_2(x,z), \text{ where}$$
$$\beta = \left((2b+x)^2 + 4z^2\right)^2. \quad (1)$$

2. The perfect square factor $\beta = 0$ does not have any real intersection with the circle $C(x,z) = 0$ traced by $\boldsymbol{p}_{c_1}$, except when $z = 0$. This special case has been discussed in Section 4.
3. The factors $O_i(x,z)$ describe *quad-circular octic curves*. The FK problem, therefore, reduces largely to the computation of the intersection of the curves $O_i(x,z)$ with the circle $C(x,z) = 0$. It is also known that the *constraint ideal* $\langle O_i, C\rangle$ defines the ith *operation mode* of the manipulator [7].

The above geometric description of the FK problem of the 3-RPS manipulator is analysed further in this work, from the perspective of *special situations*, as explained in the following section.

3. Special points at the intersection of the octic curves with the circle

Ordinarily, the octic curves $O_i = 0$ are completely disjoint, i.e., in general, the modes are independent of each other. Furthermore, $O_i = 0$ intersect the circle $C = 0$ at *distinct* points, each such point leading to an *assembly mode* of the manipulator, inside the ith operation mode. However, there are special cases, where it is possible for $O_1 = 0$, $O_2 = 0$ and $C = 0$ to share common point(s), and so on. Some of these cases are discussed in the following. It may be noted that a complete, exhaustive geometric study of all the special cases, and their mathematical/physical consequence is beyond the scope of the current work, and is a subject matter of ongoing research.

In the following, three special cases of interest are described:

1. *Points of tangency*, S_1: The circle $C = 0$ is tangent to one of the octic curves $O_1 = 0$ or $O_2 = 0$.
2. *Transition points*, S_2: The octic curves $O_1 = 0$ and $O_2 = 0$ share a common point, and the circle $C = 0$ also passes through this point.
3. *Double points*, S_3: One (or both) of the octic curves has a double point, and the circle $C = 0$ passes through this point.

A detailed description of these three geometric cases, and their kinematic consequence are presented in the Sections 3.1, 3.2 and 3.3, respectively.

3.1. Points of tangency, S_1

The point $\boldsymbol{p}_t = [x_t, z_t]^\top$ is a *double root*, when the octic curve $O_i = 0$ of the operation mode i and the circle $C = 0$, share a common tangent at the said point. One pair of double roots indicate a merger of a pair of forward kinematic branches of the manipulator.

The algebraic conditions for the curves $C = 0$, $O_i = 0$ to have a common tangent at their intersection point $\boldsymbol{p}_t$ are:

1. The said curves should pass through the *simple* point $\boldsymbol{p}_t$, implying:

$$C(x_t, z_t) = 0, \quad (2)$$
$$O_i(x_t, z_t) = 0. \quad (3)$$

2. The tangents of the curves $C = 0$, $O_i = 0$ should have the same slopes at the intersection point $\boldsymbol{p}_t$:

$$\left.\frac{\partial C}{\partial x}\right|_{\boldsymbol{p}_t}\left.\frac{\partial O_i}{\partial z}\right|_{\boldsymbol{p}_t} - \left.\frac{\partial C}{\partial z}\right|_{\boldsymbol{p}_t}\left.\frac{\partial O_i}{\partial x}\right|_{\boldsymbol{p}_t} = 0, \quad (4)$$
$$\Rightarrow z_t h_i(x_t, z_t) = 0. \quad (5)$$

The algebraic condition for tangency in Eq. (4) reduces to Eq. (5), in which the polynomial $h(x_t, z_t)$ is of degree 6 in x_t, z_t. The condition $z_t = 0$ is a very special one, which aligns the tangent at the point $\boldsymbol{p}_t$ with the axis X_A itself. This special case is not discussed in detail due to want of space; however, one example of such a situation, where the manipulator can have finite self-motions, is discussed in Section 4.

The variety S_1 is expressed in the architecture parameters a, b, and the active joint variables l_1, l_2, l_3, after eliminating x_t, z_t from Eqs. (2, 3, 5). First, z_t is eliminated, as shown in the schematics (6) and (7):

$$\left.\begin{matrix} O_i(x_t,z_t)=0 \\ C(x_t,z_t)=0 \end{matrix}\right) \xrightarrow{\times z_t} \; f_{1_i}(x_t)=0, \tag{6}$$

$$\left.\begin{matrix} h_i(x_t,z_t)=0 \\ C(x_t,z_t)=0 \end{matrix}\right) \xrightarrow{\times z_t} \; f_{2_i}(x_t)=0. \tag{7}$$

These steps result in two polynomials $f_{1_i}(x_t)$, $f_{2_i}(x_t)$ of degree 4 and 3 in x_t, respectively. The symbol '$\xrightarrow{\times z_t}$' denotes the elimination of the variable z_t from the polynomial equations preceding it.

The eliminant E_1 is obtained on eliminating the variable x_t from the polynomial equations $f_{1_i}=0, f_{2_i}=0$, as shown in the schematic (8).

$$\left.\begin{matrix} f_{1_i}(x_t)=0 \\ f_{2_i}(x_t)=0 \end{matrix}\right) \xrightarrow{\times x_t} \; E_{1_i}=0, \tag{8}$$

The eliminant E_{1_i} splits into a number of factors:

$$\begin{aligned} E_{1_i} =& (l_1-l_2)^2(l_1+l_2)^2(l_1-l_3)^2(l_1+l_3)^2(l_2-l_3)^2 \\ & \times (l_2+l_3)^2\, \zeta_i(a,b,l_2,l_3)\, \tau_i(a,b,l_1,l_2,l_3),\ i=1,2. \end{aligned} \tag{9}$$

The factors $(l_j - l_k)^2$ can be ignored, since by themselves, they *do not necessarily* imply tangency between curves intersecting at $\boldsymbol{p}_t$. The factor ζ_i in Eq. (9) being the leading co-efficient of the polynomial $f_{1_i}(x_t)$, its vanishing signifies the break-down of the elimination process depicted in the schematic (8), hence $\zeta_i = 0$ is also ignored in the following. The remaining factor, τ_i, is of degree 24 in l_1, l_2, l_3.

The polynomials τ_1, τ_2 describing the two operation modes exhibit a functional relation:

$$\tau_1(a) = \tau_2(-a). \tag{10}$$

This is analogous with the relation $g_1(a) = g_2(-a)$ between the two factors g_1, g_2 of the *forward kinematic univariate* (FKU) of the manipulator, reported in [5]. Together, these conditions signify that the π-screw motion mentioned in [7] is equivalent to the *inversion* of the top platform.

An example of such a case is obtained for the parameter values[2] $a = 9/5, b = 1, l_1 = -41/10, l_2 = 23/10, l_3 = 5.262$. The octic curves $O_1 = 0$, $O_2 = 0$ and the circle $C = 0$ are shown for these numbers in Fig. 3. As can be seen in the figure, the curve O_1 is tangential to the circle $C = 0$ at $\boldsymbol{p}_t$. The line $z = 0$ acts as a mirror plane of symmetry, as mentioned in [3].

Since the tangency implies the merger of two pairs (counting the mirror image) of FK solutions, this condition implies a *gain-type* or FK singularity of the manipulator. The corresponding pose of the manipulator along with the branches that are merging is presented in Fig. 4.

[2]All the length parameters/variables are dimensionless in this paper, as these have been scaled by the circumradius of the fixed platform, b, without any loss of generality. All angles are measured in radians, unless mentioned explicitly otherwise.

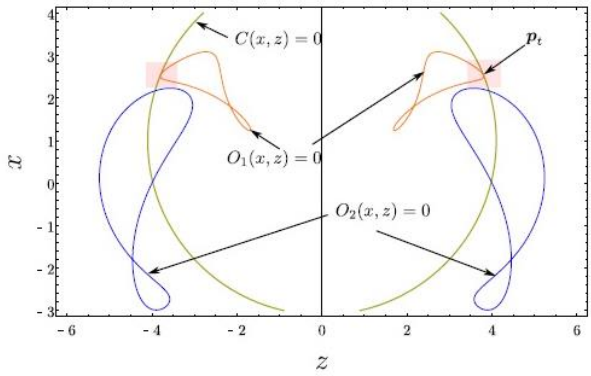

Fig. 3: Plot of the octic curves $O_1 = 0$, $O_2 = 0$ and the circle $C = 0$ for the tangency condition $\tau_1 = 0$.

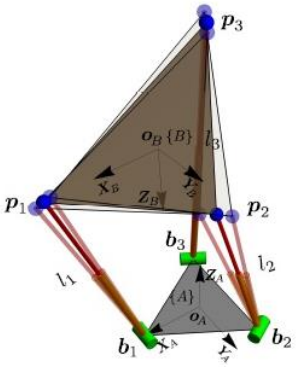

Fig. 4: Singular pose of the 3-RPS manipulator where the FK branches merge.

3.2. Points of transition, S_2

A point $\boldsymbol{p}_m = [x_m, z_m]^\top$ denotes the *transition point* between the operation modes, when it is at the intersection of the octic curves $O_1(x,z) = 0$, $O_2(x,z) = 0$, as well as the circle $C(x,z) = 0$. Hence, the following conditions define such a point:

$$C(x_m,z_m)=0,\ O_1(x_m,z_m)=0,\ O_2(x_m,z_m)=0. \tag{11}$$

As in the case of S_1, the variety S_2 is obtained in the variables l_i, and the parameters a, b, after the elimination of x_m, z_m from Eq. (11). The elimination process is briefly described in the following schematics:

$$\left.\begin{matrix} O_1(x_m,z_m)=0 \\ C(x_m,z_m)=0 \end{matrix}\right) \xrightarrow{\times z_m} \; f_3(x_m)=0, \tag{12}$$

$$\left.\begin{matrix} O_2(x_m,z_m)=0 \\ C(x_m,z_m)=0 \end{matrix}\right) \xrightarrow{\times z_m} \; f_4(x_m)=0. \tag{13}$$

The resultant of f_3 and f_4 w.r.t. x_m results in the eliminant E_2 as depicted in the schematic (14):

$$\left.\begin{matrix} f_3(x_m)=0 \\ f_4(x_m)=0 \end{matrix}\right) \xrightarrow{\times x_t} \; E_2=0. \tag{14}$$

The eliminant E_2 splits into five factors:

$$E_2 = a^4\, \xi_1 \xi_2 \xi_3 \xi_4 = 0. \tag{15}$$

The polynomials $\xi_1, \xi_2, \xi_3, \xi_4$ are of degree 8, 8, 8 and 24, respectively, in the variable l_1, l_2, l_3. It is verified that each of these factors admit real solutions. Some of these real solutions are analysed numerically and geometrically, from which the following observations emerge:

1. Only the vanishing of ξ_3 corresponds to the condition for the transition point between the operation modes. It is verified, numerically, that such transition points are singular as well, as mentioned in [7].
2. The conditions $\xi_1 = 0$, $\xi_2 = 0$ cause two *distinct non-singular* poses of the manipulator, belonging to distinct operation modes, to have one of the sides of the moving platform in common. Such a situation is depicted in Fig. 8, where the side $\boldsymbol{p}_1\boldsymbol{p}_3$ is common between the operation modes of the manipulator. In this work, the sides involved can only be $\boldsymbol{p}_1\boldsymbol{p}_2$ or $\boldsymbol{p}_1\boldsymbol{p}_3$, since the manipulator was broken at this point for the present analysis.
3. The equation $\xi_4 = 0$ describes the condition for two *distinct non-singular* poses of the manipulator belonging to distinct operation modes to have a point in common. For reasons explained above, the said point can only be $\boldsymbol{p}_1$ in this work.

From these observations, it appears that the factors 2 and 3 are artefacts of the resultant-based elimination process. For the above said reasons cases 2, 3 do not represent a transition.

The polynomial ξ_3 being symmetric in l_1, l_2, l_3, distinguishes itself from the others in Eq. (15). Similarly, the polynomials ξ_2, ξ_1 are symmetric in l_2, l_3 and the polynomial ξ_4 is not symmetric in any of the input joint parameters l_1, l_2 or l_3.

It is important to note here that the observations made above are based on numerical examples, and not exhaustive mathematical analysis. Hence, interesting as they are, they can only hoped to be indicative at this point.

An example for the case where $\zeta_3 = 0$ is obtained for the parameter values $a = 1/2$, $b = 1$, $l_1 = 22/10$, $l_2 = 23/10$, $l_3 = 2.936$. For these values, the curves $O_1 = 0$, $O_2 = 0$, $C = 0$ meet at a common point $\boldsymbol{p}_{m_1}$ as depicted in Fig. 5. This point $\boldsymbol{p}_{m_1}$ represents the transition point between the operation modes of the manipulator.

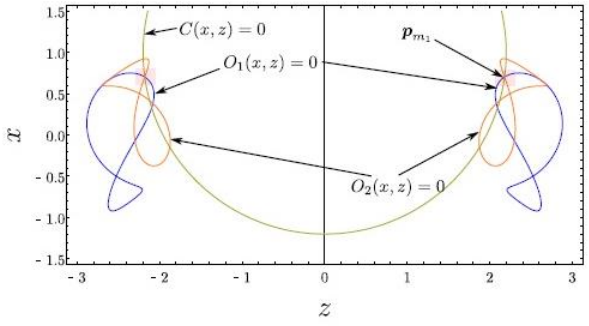

Fig. 5: Plot of the octic curves $O_1 = 0$, $O_2 = 0$, circle $C = 0$ for $\xi_3 = 0$.

The singular pose of the manipulator at this transition point $\boldsymbol{p}_{m_1}$ is shown in Fig. 6. The fixed and moving platforms of the manipulator are in parallel planes with the latter flipped by π w.r.t to the former. A similar configuration is reported as the constraint singularity of the 3-RPS manipulator in [9] and as the transition between the operation modes $x_0 = 0, x_1 = 0$ in [10].

An example for the case, where the octic curves $O_1 = 0$, $O_2 = 0$, and the circle $C = 0$ meet at a common point $\boldsymbol{p}_{m_2}$ for the values of

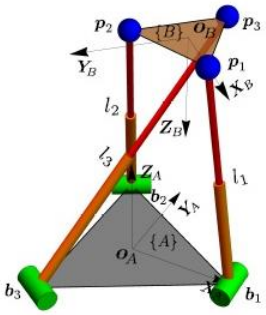

Fig. 6: Pose of the 3-RPS manipulator at the transition.

the parameters $b = 1$, $l_1 = 22/10$, $l_2 = 23/10$, $l_3 = 1.930$ satisfying $\zeta_1 = 0$ is shown in Fig. 7. This point $\boldsymbol{p}_{m_2}$ does not represent a transition point for the above discussed reasons.

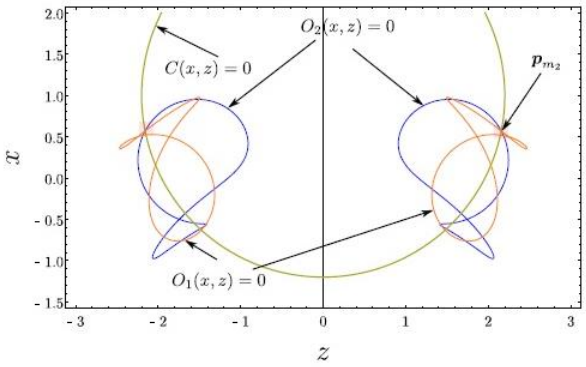

Fig. 7: Plot of the octic curves $O_1 = 0, O_2 = 0$ and the circle $C = 0$ for $\xi_1 = 0$.

The corresponding *non-singular* poses of the manipulator at the point $\boldsymbol{p}_{m_2}$ are as depicted in Fig. 8. Clearly, these are two different poses of the manipulator except for the common side $\boldsymbol{p}_3\boldsymbol{p}_1$.

3.3. Double points of the octic at the intersection with the circle, S_3

Another interesting class of special points are the *double points* on either $O_1 = 0$ or $O_2 = 0$, when the circle $C = 0$ also passes through it. Since the said curves are octic in nature, there can be up to four pairs of double points on each (e.g., the points at infinity in each). However, in this work, only one pair of double points is considered due to space constraints. According to [4], pp. 2, "A *double point* of a curve is a point P such that *every* line through P meets the curve *twice* at P". These are further classified as *infinite* and *finite* double points, depending upon whether they are at infinity, or not.

3.3.1. Finite double points

The conditions for obtaining a finite double point, denoted by $\boldsymbol{p}_d = [x_d, z_d]^\top$, on the octic curve $O_i = 0$ intersecting with the circle $C = 0$ are:

1. The gradient of the octic curve $O_i = 0$ along x, z at the point $\boldsymbol{p}_d$ should be zero. Therefore, $\boldsymbol{p}_d$ is a double point of the octic

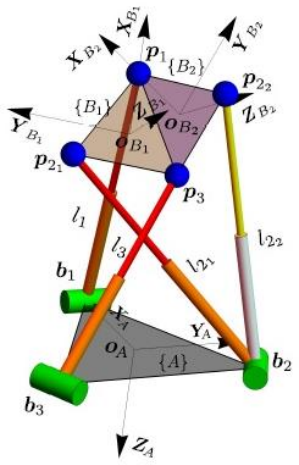

Fig. 8: Non-singular distinct poses of the 3-RPS manipulator.

curve $O_i = 0$, provided:

$$O_i(x_d, z_d) = 0, \left(\frac{\partial O_i}{\partial x}, \frac{\partial O_i}{\partial z}\right)^{\top}_{\boldsymbol{p}_d} = \mathbf{0}. \tag{16}$$

2. The double point $\boldsymbol{p}_d$ is required to lie on the circle $C = 0$ as well:

$$C(x_d, z_d) = 0. \tag{17}$$

As in the case of S_2, the variety S_3 is obtained by first eliminating the variables x_d, z_d from the Eqs. (16, 17), to obtain an equation in the parameters a, b, and the variables l_1, l_2, l_3. The elimination process is briefly described by the following schematics:

$$\left.\begin{matrix} O_i(x_d, z_d) = 0 \\ C(x_d, z_d) = 0 \end{matrix}\right) \xrightarrow{\times z_d} f_{5_i}^2(x_d) = 0, \tag{18}$$

$$\left.\begin{matrix} \frac{\partial O_i}{\partial x}\Big|_{\boldsymbol{p}_d} = 0 \\ C(x_d, z_d) = 0 \end{matrix}\right) \xrightarrow{\times z_d} f_{6_i}^2(x_d) = 0, \tag{19}$$

$$\left.\begin{matrix} \frac{\partial O_i}{\partial z}\Big|_{\boldsymbol{p}_d} = 0 \\ C(x_d, z_d) = 0 \end{matrix}\right) \xrightarrow{\times z_d} (b - l_1 - x_d)(b + l_1 - x_d) f_{7_i}^2(x_d) = 0. \tag{20}$$

The polynomials $f_{5_i}, f_{6_i}, f_{7_i}$ are of degree 4, 4 and 3 in x_d, respectively. The factors preceding the equation $f_{7_i} = 0$ in Eq. (20) correspond to the case when $z_d = 0$, the details of which are discussed in Section 4. The resultant of the polynomial equations $f_{5_i} = 0, f_{6_i} = 0$ with the equation $f_{7_i} = 0$ in x_d, results in two polynomials r_{1_i}, r_{2_i} in the parameters a, b, l_1, l_2, l_3 as depicted in the schematics (21, 22).

$$\left.\begin{matrix} f_5 = 0 \\ f_7 = 0 \end{matrix}\right) \xrightarrow{\times z_d} r_{1_i} = 0, \tag{21}$$

$$\left.\begin{matrix} f_6 = 0 \\ f_7 = 0 \end{matrix}\right) \xrightarrow{\times z_d} r_{2_i} = 0. \tag{22}$$

Once again, it may be noted that the expressions for r_{1_i}, r_{2_i} for the two operation modes vary only by the sign of the parameter a, i.e.:

$$r_{1_i}(a) = r_{2_i}(-a). \tag{23}$$

Furthermore, r_{1_i}, r_{2_i} factorises as shown in Eqs. (24, 25), respectively:

$$\begin{aligned} r_{1_i} =& (l_1 - l_2)^2 (l_1 + l_2)^2 (l_1 - l_3)^2 (l_1 + l_3)^2 (l_2 - l_3)^2 \\ & \times (l_2 + l_3)^2 \, \delta_i(a, b, l_1, l_2, l_3) = 0, \end{aligned} \tag{24}$$

$$\begin{aligned} r_{2_i} =& (a - 2b)(l_1 - l_2)^2 (l_1 + l_2)^2 (l_1 - l_3)^2 (l_1 + l_3)^2 \\ & \times (l_2 - l_3)^2 (l_2 + l_3)^2 \, (3a^2 - 6ab - 6b^2 - {l_2}^2 - {l_3}^2) \\ & \times \mu_i(a, b, l_1, l_2, l_3) = 0. \end{aligned} \tag{25}$$

The polynomials δ_i, μ_i in Eqs. (24, 25) are each of degree 24 in the variables l_1, l_2, l_3.

The factors $(l_j - l_k)^2$ represent the symmetry in the kinematic sub-chains of the manipulator. In particular, when $l_2 = l_3$ the octic curves split into a pair of coincident circles and a quartic curve (shown in Fig. 11). As mentioned in Section 3.1, these do *not necessarily* enforce the tangency between the circle and the octic curve, but the octic curve intersects the circle at the double point.

At a double point $\boldsymbol{p}_d$ of the octic curve $O_i = 0$, the equation of the *tangents* is given by:

$$\begin{aligned} t_{o_i} =& \frac{\partial^2 O_i}{\partial^2 x}\Big|_{\boldsymbol{p}_d} (x - x_d)^2 + 2 \frac{\partial^2 O_i}{\partial x \partial z}\Big|_{\boldsymbol{p}_d} (x - x_d)(z - z_d) \\ & + \frac{\partial^2 O_i}{\partial^2 z}\Big|_{\boldsymbol{p}_d} (z - z_d)^2 = 0. \end{aligned} \tag{26}$$

The discriminant Δ of the quadratic equation given in Eq. (26) is:

$$\Delta = \frac{\partial^2 O_i}{\partial^2 x}\Big|_{\boldsymbol{p}_d} \frac{\partial^2 O_i}{\partial^2 z}\Big|_{\boldsymbol{p}_d} - \left(\frac{\partial^2 O_i}{\partial x \partial z}\Big|_{\boldsymbol{p}_d}\right)^2. \tag{27}$$

Based on the value of this discriminant Δ, the double point $\boldsymbol{p}_d$ is qualified to be any one of the following:

1. A *crunode* $\boldsymbol{p}_{n_1}$: There exists two distinct tangents at this point and the discriminant is less than zero ($\Delta < 0$).
2. An *acnode* $\boldsymbol{p}_{n_2}$: The equation of the tangents $t_{o_i} = 0$ does not admit any real solutions as the discriminant is greater than zero ($\Delta > 0$). Hence, there are no tangents at this point.
3. A *cusp* $\boldsymbol{p}_c$: The two tangents at this point coincide as the discriminant is zero ($\Delta = 0$).

An example for case 3, where a cusp $\boldsymbol{p}_c$ occurs at the intersection of $O_1 = 0$ with the circle $C = 0$ for the following numerical values: $a = 2$, $b = 1$, $l_1 = -29/10$, $l_2 = 29/10$, $l_3 = \frac{(-30-\sqrt{1141})}{10}$ is shown in the Fig. 9. The corresponding pose of the manipulator is shown in Fig. 10.

As can be seen from the Fig. 10, the pose of the manipulator is special from multiple perspectives:

1. The third leg lies in the plane of the moving platform.
2. The lines joining the spherical joints $\boldsymbol{p}_3, \boldsymbol{p}_2$ and $\boldsymbol{p}_3, \boldsymbol{p}_1$ intersect the axis of the rotary joint at $\boldsymbol{b}_3$. This pose exemplifies case 2 of the singularity conditions of the manipulator, as presented in [8]. The same configuration has been characterised under *constraint singularity* in [9].
3. The axes of all the three legs intersect the line $\boldsymbol{p}_1\boldsymbol{p}_2$.

The kinematic consequence of this condition is that the manipulator is singular. However, it is also possible to have a situation, where the circle $C = 0$ intersects one of the octic curves at a double point, but the manipulator is *not* singular. Such a configuration is obtained for the following set of values: $l_2 = l_3 = 1$, $l_1 = 3/2$, $a = 1/2$ $b = 1$. In this case $O_1 = 0$ splits into two components, i.e., $O_1 = O_{1a} O_{1b} = 0$, which have the following nature:

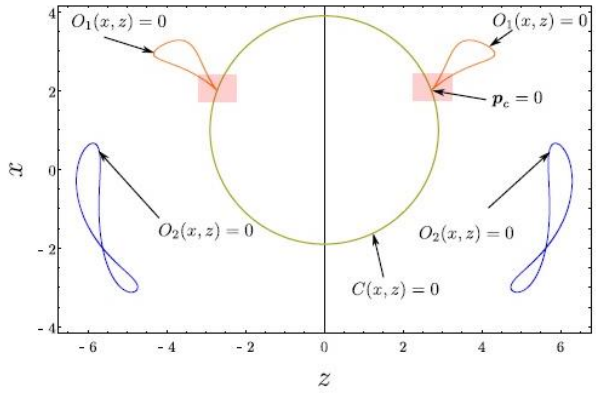

Fig. 9: Plot of the octic curves $O_1 = 0$, $O_2 = 0$ and the circle $C = 0$ at $a = 2b$, $l_1 = l_2$ and $\mu_1 = 0$.

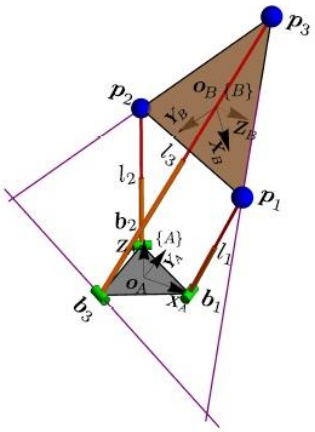

Fig. 10: Singular pose of the 3-RPS manipulator at the cusp p_c.

1. The curve $O_{1a} = 0$ is a pair of *coincident* circles, shown in solid (blue) line-type in Fig. 11.
2. The curve $O_{1b} = 0$ decomposed into two components, each being a circle, shown in dashed (blue) line-type in Fig. 11.

Similarly, the curve $O_2 = 0$ splits into two quartic curves $O_{2a} = 0$, $O_{2b} = 0$, whose nature is:

1. The curve $O_{2a} = 0$ further decomposes to a pair of *coincident circles* shown in dotted (orange) line-type in Fig. 11.
2. The other quartic curve $O_{2b} = 0$ does not admit any real solution.

Clearly, any intersection of $O_{1a} = 0$ with $C = 0$ would be a double point of the former. However, it can be verified, that this double point does not signify a singularity. The poses of the manipulator corresponding to point p_{d_1} in Fig. 11 are shown in Fig. 12. It can be seen that only the vertex p_1 is the same between the two poses, but that is not enough to cause a singularity in the manipulator.

3.3.2. Double points at infinity

In order to study the double points at infinity, one needs to resort to the use of projective/homogeneous coordinates. Let w be the *homogenising coordinate*, so that the projective versions of the octic

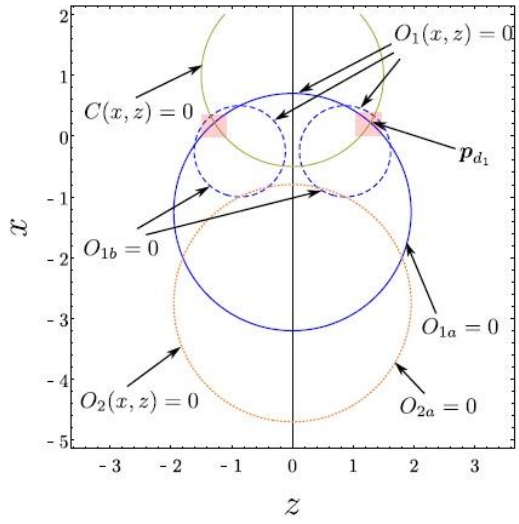

Fig. 11: Plot of the octic curves $O_1 = 0, O_2 = 0$ and the circle $C = 0$ at the double point satisfying $l_2 = l_3$.

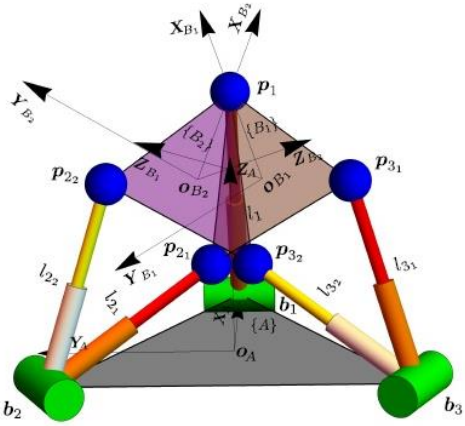

Fig. 12: Non-singular poses of the 3-RPS manipulator at the double point satisfying $l_2 = l_3$.

curves can be written as $O_{h_i}(X,Z,w) = 0$, where:

$$X = \frac{x}{w},\ Z = \frac{z}{w}. \tag{28}$$

In this framework, a double point p_h can be expressed as $p_h = [x_h, z_h, w]^\top$. The point p_h becomes a double point at infinity, when the gradient of $O_{h_i} = 0$ w.r.t. $[X,Z,w]^\top$ vanishes at p_h, and in addition, $w = 0$:

$$\begin{aligned} &\left.\frac{\partial O_{h_i}}{\partial X}\right|_{p_h,w=0} = 0,\ \left.\frac{\partial O_{h_i}}{\partial w}\right|_{p_h,w=0} = 0,\ \left.\frac{\partial O_{h_i}}{\partial Z}\right|_{p_h,w=0} = 0, \\ &\Rightarrow 8x_h\left(x_h^2+z_h^2\right)^3 = 0,\ 4(a-2b)x_h\left(x_h^2+z_h^2\right)^3 = 0, \text{ and} \\ &\quad 8z_h\left(x_h^2+z_h^2\right)^3 = 0. \end{aligned} \tag{29}$$

The only real solution to Eq. (29) is $x_h = 0$, $z_h = 0$, $w = 0$, which is not included in the projective space. The result supports the fact that the quad-circular octic curve $O_i = 0$ do not have asymptotes.

4. Special case of $z = 0$

At several places in the previous sections, $z = 0$ came up as a special case, the discussions on which have been deferred to this section. As may be expected, the implication of this additional condition varies from one case to the other. Some of these are discussed in the following.

4.1. Implication of $z = 0$ in the FK problem

In Eq. (1) of Section 2 it was shown that the FK problem of the 3-RPS manipulator is equivalent to the intersection of a curve $\alpha(x,z) = 0$ with a circle in the same vertical plane, where one of the components of the said curve is given by:

$$\beta(x,z) = \left((2b+x)^2 + 4z^2\right)^2 = 0. \tag{30}$$

The only real solution to the problem is: $x = -2b$, $z = 0$. Since the circle $C = 0$ needs to pass through this point, given by, say, $\boldsymbol{p}_a = [-2b, 0]^\top$, one can write:

$$C(x,y)_{\boldsymbol{p}_a} = 0 \Rightarrow {l_1}^2 - 9b^2 = 0. \tag{31}$$

At point $\boldsymbol{p}_a$ the octic curve $O_i = 0$ admits a real solution when:

$$O_i(x,y)_{\boldsymbol{p}_a} = 0 \Rightarrow l_2^2 = 3a^2 - 3b^2,\ l_3^2 = 3a^2 - 3b^2. \tag{32}$$

Clearly, the solution is independent of the operation mode of the manipulator. The conditions in Eqs. (31, 32) lead to *finite self-motions* in the 3-RPS manipulator, as reported in [11]. Interestingly, the point $\boldsymbol{p}_a$ is an *acnode* of the curve $\beta = 0$. For the numeric values $a = 3/2$, $b = 1$, $l_1 = 3$, $l_2 = \sqrt{15}/2$, $l_3 = \sqrt{15}/2$ that satisfy Eqs. (31, 32), the plots of the curves are shown in Fig. 13.

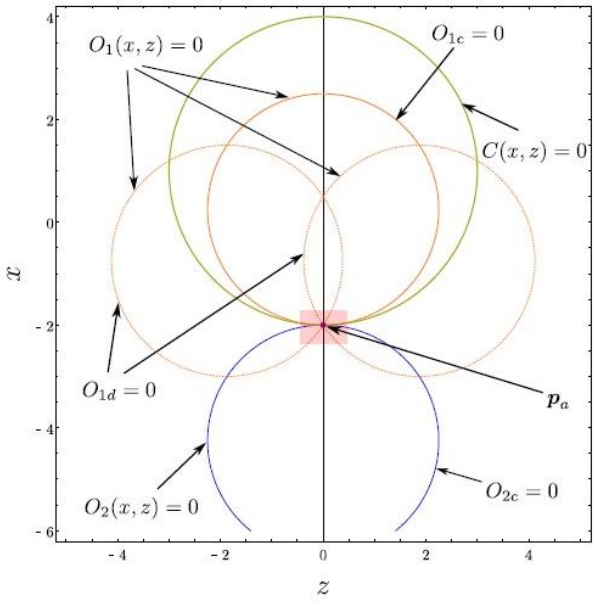

Fig. 13: Plot of the octic curves $O_1 = 0$, $O_2 = 0$, the circle $C = 0$ intersecting at the acnode of the curve $\beta = 0$.

The octic curve $O_1 = 0$ splits into $O_1 = O_{1c}O_{1d} = 0$ and the nature of these curves are:

1. The curve $O_{1c} = 0$ is a pair of coincident circles, as depicted in solid (orange) line-type in Fig. 13. This pair is tangent to the circle $C = 0$ at the *tacnode* $\boldsymbol{p}_a$.
2. The component $O_{1d} = 0$ further decomposes to two circles as shown in dotted (orange) line-type in Fig. 13. Each of these circles intersect the circle $C = 0$ at the point $\boldsymbol{p}_a$.

The curve $O_2 = 0$ splits into two factors $O_2 = O_{2c}O_{2d} = 0$, whose nature is:

1. Similar to the curve $O_{1c} = 0$, $O_{2c} = 0$ is also a pair of *concentric circles* represented in solid (blue) line-type in Fig. 13. This pair is tangent to the circle $C = 0$ at the point $\boldsymbol{p}_a$.
2. The curve $O_{2d} = 0$ admits two repeated real solutions at the point $\boldsymbol{p}_a$, hence the said point is an *acnode* of this curve.

The curve $\beta = 0$ has an *acnode* at $\boldsymbol{p}_a$ highlighted by a translucent rectangle, as shown in Fig. 13.

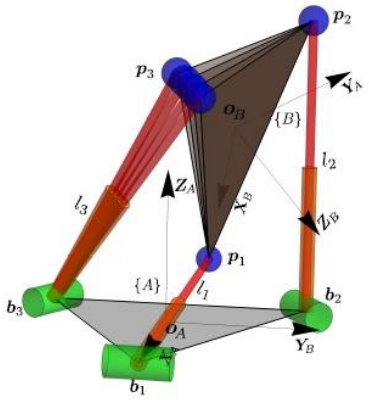

Fig. 14: Finite self-motion of the manipulator at the point $\boldsymbol{p}_a$.

The manipulator is known to exhibit finite self-motion in this case and this corresponds to the case 2(a) reported in [11]. For the given input parameters $\boldsymbol{l}$, maintaining the position of the point $\boldsymbol{p}_1$ the RSSR sub-chain exhibits the finite self-motion as shown in Fig 14.

5. Conclusion

In this paper, the special cases in the forward kinematics of the 3-RPS manipulator are analysed, using only the concepts of geometry of plane curves. It turns out that this technique is as powerful, as it is intuitive. It has been able to recover results in existing literature, which have been obtained using algebraic means. Moreover, it has been able to associate geometric implications to each of these cases, e.g., singularities, transitions between modes, finite self-motions, etc. These special cases have been studied via numerical examples, the results of which have been tabulated in Table 1. The table suggests that the geometric condition for singularity in Basu and Ghosal [8] may be geometrically equivalent to an octic curve intersecting a circle at a cusp. Similarly, the finite self-motion of the manipulator may be associated with the a quadratic curve having an acnode on the same circle. It needs to be noted, however, that these results are by no means exhaustive. While they hint at various possibilities, they need to be studied in depth, analytically, in order to establish the inter-relationships between various geometric conditions, their algebraic implications, and kinematic consequences. It is definitely worth undertaking such a study, as there are multiple spatial manipulators whose kinematics are fairly *similar* to that of the 3-RPS manipulator, namely, the 3-RRS, MaPaMan-I, 3-RPRS. A thorough understanding of the kinematics of the 3-RPS should help develop significant understanding of the kinematics of these manipulators as well.

Table 1: Relationships between various geometric conditions and their kinematic consequences.

Σ^1 : The algebraic conditions for the *gain-type* singularity of the 3-RPS manipulator discussed in [7],
B : Case 2 of the geometric condition of singularity of the 3-RPS manipulator reported in [8],
D : A double root of the FKU defined in Stüdy parameters,
P : The condition for any one of the legs of the 3-RPS manipulator co-planar with the moving platform.

Figure	Examples	Σ^1	B	D	P
3	The octic curve $O_i = 0$ is tangent to the circle $C = 0$.	✓	×	✓	×
5	The curves $O_1 = 0, O_2 = 0$, $C = 0$ intersect at a point. Transition between the operation modes	✓	×	✓	×
7	The octic curves $O_1 = 0$, $O_2 = 0$ have a common point on the circle $C = 0$. Two distinct poses share a common side of the moving platform.	×	×	×	×
9	A cusp of the octic curve $O_i = 0$ appears on the circle $C = 0$.	✓	✓	✓	✓
11	A double pointof the octic curve $O_i = 0$ occurs on the circle $C = 0$ and the RSSR sub-chain is symmetric.	×	×	×	×
13	An acnode of the curve $\beta = 0$ appears on the circle $C = 0$. Manipulator exhibits finite self-motion.	✓	×	✓	×

References

[1] J. A. Hrones and G. L. Nelson, *Analysis of the Four-bar Linkage*. New York: The Technology Press of the Massachusetts Institute of Technology and John Wiley & Sons, Inc., 1951.

[2] K. Hunt, "Structural kinematics of in-parallel-actuated robot-arms," *Journal of Mechanisms, Transmissions, and Automation in Design*, vol. 105, no. 4, pp. 705–712, 1983.

[3] T. K. Mamidi, A. Baskar, and S. Bandyopadhyay, "A novel geometric analysis of the kinematics of the 3-RPS manipulator," *Accepted to be presented in 7th IFToMM International Workshop on Computational Kinematics*, (Futuroscope-Poitiers), 2017.

[4] E. J. F. Primrose, *Plane Algebraic Curves*. MacMillan & Co Ltd., 1955.

[5] R. A. Srivatsan and S. Bandyopadhyay, "Analysis of constraint equations and their singularities," in *Advances in Robot Kinematics*, pp. 429–436, Springer, 2014.

[6] V. I. Arnold, S. M. Gusein-Zade, and A. N. Varchenko, *Singularities of Differentiable Maps, Volume 1*. Boston: Birkhüser, 1985.

[7] J. Schadlbauer, D. Walter, and M. Husty, "The 3-RPS parallel manipulator from an algebraic viewpoint," *Mechanism and Machine Theory*, vol. 75, pp. 161–176, 2014.

[8] D. Basu and A. Ghosal, "Singularity analysis of platform-type multi-loop spatial mechanisms," *Mechanism and Machine Theory*, vol. 32, pp. 375–389, April 1997.

[9] D. Zlatanov, I. A. Bonev, and C. M. Gosselin, "Constraint singularities of parallel mechanisms," in *International Conference on Robotics and Automation*, (Washington D.C), pp. 496–502, May 2002.

[10] J. Schadlbauer, D. Walter, and M. Husty, "A complete kinematic analysis of the 3-RPS parallel manipulator," in *15th National Conference on Machines and Mechanisms*, (Indian Institute of Technology Madras, Chennai), pp. 1–10, 2011.

[11] J. Schadlbauer, M. L. Husty, S. Caro, and P. Wenger, "Self-motions of 3-RPS manipulators," *Frontiers of Mechanical Engineering*, vol. 8, no. 1, pp. 62–69, 2013.